Delayed fission

V. I. Kuznetsov

Joint Institute for Nuclear Research, Dubna
Fiz. Elem. Chastits At. Yadra **12**, 1285–1323 (November–December 1981)

The experimental investigations of nuclei whose daughter products after K capture or β^- decay undergo fission from an excited state (delayed fission) are reviewed. The main theoretical ideas about the process of delayed fission, the possibility of determining the heights of the fission barriers from the measured probabilities p_{df}, and the part played by delayed fission in nucleosynthesis in pulsed neutron fluxes and the r process are considered.

PACS numbers: 24.75. + i, 27.90. + b

INTRODUCTION

With increasing neutron deficit or excess the β-decay energy Q_β of heavy nuclei becomes comparable with the height of the fission barrier or even exceeds it. As a rule, β decay takes place to not only the ground state but also higher levels of the final nucleus. In contrast to α decay, the energy of the excited levels is not necessarily low, and may, in fact, be comparable with the total energy Q_β. Thus, in some cases the excitation energy E of the daughter nucleus after decay to a high-lying level is sufficient for fission to occur. By analogy with the emission of delayed protons and neutrons, such a process has been called delayed fission.[1]

Delayed fission was discovered for the first time in an attempt to synthesize spontaneously fissioning shape isomers in the region of neutron-deficient nuclei.[2] Subsequently, nuclei that undergo delayed fission were identified in reactions in heavy-ion beams.[1,3,4]

Experimental observation of delayed fission is possible if the probabilities of the competing processes of de-excitation of the daughter nucleus, namely, the emission of γ rays and delayed neutrons, are of the same order as, or less than, the fission probability. These conditions are ensured when the probability $b(E)$ of population of the levels of the daughter nucleus is fairly high in the region of energies B_f. The probabilities of β and α decay of the parent nucleus must also be of the same order.

The conditions for experimental observation of delayed fission are most frequently satisfied for odd–odd nuclei. The large Q_β compared with neighboring nuclei due to the odd–even effect and the high fissility of the even–even daughter nucleus have the consequence that Q_β and B_f are comparable even at a relatively small distance from the line of β stability. The high neutron separation energy B_n of the daughter nucleus reduces the competition from emission of delayed neutrons for neutron-rich nuclei. In addition, the density of the low-lying levels of the even–even daughter nucleus is low, which facilitates population of the high-lying levels. The region of nuclei in which delayed fission is energetically possible[5] is shown in Fig. 1.

Study of delayed fission opens up new ways to investigate nuclei far from the β-stability line. Thus, experimental data on the probabilities of delayed fission characterize the parameters of the fission barriers, the quantities that determine the stability of a nucleus with respect to spontaneous fission, its fissility at low excitation energies, and so forth.

At the present time, the parameters of the fission barriers are measured in induced-fission reactions at low excitation energies and in synthesis reactions of spontaneously fissioning isomers. However, these methods are inapplicable for nuclides at a significant distance from the β-stability line— either because there are no spontaneously fissioning isomers, or because of the impossibility of synthesizing nuclei in this region. Delayed fission is manifested in many processes, including β decay. It undoubtedly plays an important part in astrophysical processes involving the synthesis of heavy and superheavy elements. According to modern ideas, delayed fission is an important source of energy of supernovae at a definite stage of their evolution. Only allowance for delayed fission made it possible to explain and predict the synthesis of heavy elements observed in the pulsed neutron fluxes of thermonuclear explosions.

1. THEORETICAL TREATMENT. BASIC IDEAS

Delayed fission was considered qualitatively in Ref. 6. The complete description of delayed fission involves fairly complicated transitions in the participating nuclei.

The usually adopted shape of the two-hump fission barrier of a nucleus and the various transitions that lead to delayed fission are shown in Fig. 2. If the β decay results in population of levels below the fission barrier and $E_i < B_n$, where E_i is the energy of the level and B_n is the neutron separation energy, the nucleus can undergo fission, since under these conditions the

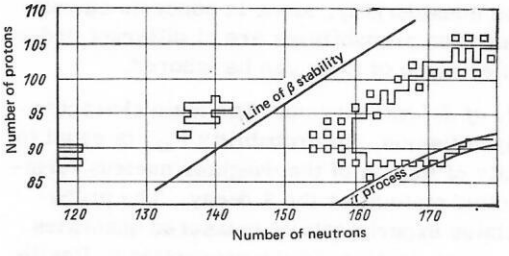

FIG. 1. Regions of delayed fission.

 0090-4759/81/060511-17$02.80

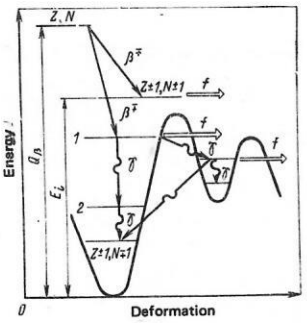

FIG. 2. Decay scheme of a nucleus in the case of delayed fission.

widths of the radiative transitions to the lower levels are appreciably less than the fission width, i.e., $\Gamma_f \gg \Gamma_\gamma$. If the relation $E_i > B_n$ holds for a given level of a neutron-rich nucleus, emission of a delayed neutron begins to compete with the fission process. As a result, the probability of fission from the level E_i is $\Gamma_f(E_i)[\Gamma_f(E_i)+\Gamma_n(E_i)]^{-1}$.

The fission process is more complicated when the energy of the excited level lies between the energy of the second barrier E_B and the energy of the second minimum E_{II}. At excitation energies in this interval, fission takes place from the states in the second potential well, as was shown by investigations on below-barrier photofission of heavy nuclei.[7] Two possibilities exist for a transition to the second potential well. After β decay, the nucleus (Z,N) goes over without significant change of deformation to a level of the first potential minimum. Then the nucleus tunnels with probability $W_\gamma^A(E)$ through the inner barrier A into the potential well II.

Another possibility is decay with a significant change in the deformation and a direct transition with probability $W_A(E)$ to the levels of the well II. If we denote by $W_B(E)$ the probability of tunneling through the barrier B, and by W_{γ_1} and W_{γ_2} the probabilities of γ transitions in the first and the second potential well, respectively, then[8]

$$\frac{\Gamma_f}{\Gamma_t}=\frac{W_A+W_\gamma^A}{W_A+W_\gamma^A+W_{\gamma_1}} \times\left(\frac{W_B}{W_A+W_B+W_{\gamma_2}+W_\gamma^A}+\frac{W_{\gamma_2}}{W_A+W_B+W_{\gamma_2}+W_\gamma^A}\frac{W_B}{W_A+W_B+W_\gamma^A}\right). \quad (1)$$

The first term on the right-hand side of (1) is the probability of transition of the nucleus to a state of the second potential well with energy E, and the expression in the brackets is the total probability of fission from the second well. In many cases, the expression (1) simplifies considerably, since in concrete calculations the transition probabilities are of different order and, as a rule, some of them can be ignored.

Probability of delayed fission. The main characteristic of delayed fission, its probability P_{df}, is equal to the probability of fission of the daughter nucleus formed in the excited state after the β decay. The probability P_{df} relates experimentally measured quantities, namely, the cross section for the production of fissile nuclei in the nuclear reaction, σ^f, to the production cross section σ and the half-lives T_α, T_β, and T_f of the parent nucleus until α and β decay and spontaneous fission:

$$\sigma_f=\sigma T_\alpha\Big(\sum_{i=\alpha,\beta} T_i\Big)^{-1} P_{df}. \quad (2)$$

The probability P_{fi} of delayed fission from the daughter-nucleus level E_i is proportional to the product of the probability $b(E_i)$ of population of this level and the ratio of its fission width $\Gamma_f(E)$ to the total width $\Gamma_t(E)$:

$$P_{f_i}=\frac{\Gamma_f(E_i)}{\Gamma_t(E_i)}\,b(E_i). \quad (3)$$

The influence of the structure of the nucleus on the β decay is described by the strength function $S_\beta(E_i)$. The probability of population $b(E)$ is related to $S_\beta(E_i)$ by

$$b(E_i)=kS_\beta(E_i)\,f(Z,\,Q_\beta-E_i). \quad (4)$$

Here, $k=T_{1/2}$, and $f(Z,Q_\beta-E_i)$ is the Fermi function which characterizes the kinematics of the β decay.

Ultimately,

$$P_{df}=\frac{\sum_i f(Z,\,Q_\beta-E_i)\,S_\beta(E_i)\,\Gamma_f(E_i)\,\Gamma_t(E_i)^{-1}}{\sum_i f(Z,\,Q_\beta-E_i)\,S_\beta(E_i)}. \quad (5)$$

Strength function. The strength function $S_\beta(E_i)$ (see Refs. 9 and 10) can be represented in the form

$$\sum_J \rho_J(E_i)\,|Mif|^2/\tau_0\ \text{MeV}^{-1}\cdot\text{sec}^{-1}, \quad (6)$$

where $|M_{if}|^2$ is the mean probability of transition to the final level f with energy E_i, $\rho_J(E)$ is the density of the levels of the daughter nucleus with spin and parity satisfying the selection rules with respect to J, and τ_0 is the universal time constant of β decay.

In the analysis of delayed fission, three assumptions are usually made about the form of $S_\beta(E)$:

1) $S_\beta(E)=\text{const}, E>C$; $S_\beta(E)=0, E<C$;

2) $S_\beta(E)\sim\rho(E)$, where $\rho(E)$ is the level density of the daughter nucleus;

3) $S_\beta(E)$ can be calculated on the basis of the gross theory of β decay.

Transitions of Fermi type are concentrated in a narrow energy interval (>0.3 MeV) in the region of the isobar-analog state, which lies at an energy around 20 MeV for heavy nuclei, i.e., appreciably higher than the excitation energies of the daughter nuclei of the actinides formed after β decay. Therefore, in the region in which we are interested Gamow–Teller transitions are either forbidden or suppressed.

To interpret the experimental data, the approximation 1 is successfully used[11,12] in the study of neutron-deficient nuclei, while the approximation 2 is successfully used for neutron-rich nuclei.[13,14] However, neither the first nor the second assumption about the form of $S_\beta(E)$ fully reflects the influence of the real nuclear structure on the matrix elements of the β transition, since the selection rules are not taken into account. The $S_\beta(E)$ determined on the basis of the gross theory of β decay is a better representation of the strength function. In this case, one does take into

account the single-particle selection rules and nuclear structure, albeit very simplified.

The existence of low-lying structures in the strength function having a considerable influence on delayed processes has recently been demonstrated,[15] and these structures have been calculated by a "microscopic" method for some nuclei in the region of the actinides.

For example, the strength function has been calculated for the Gamow–Teller β decay of ^{236}Pa and ^{238}Pa. The deformation of the nuclei ^{236}U and ^{238}U was not taken into account. The matrix of the Hamiltonian $H = H_{sp} + H_{int}$ was diagonalized numerically on a basis of single-particle proton and neutron-hole states with spin I^π. The interaction Hamiltonian is $H_{int} = \mathcal{G}_1(\sigma_1\sigma_2) \times (\tau_1\tau_2)$, where $\mathcal{G}_1$ is the coupling constant.

There are two types of collective state for Gamow–Teller β transitions that can be situated in the Q_β window, namely, core-polarization states and states of the inverse spin-flip type.

For heavy nuclei, theoretical calculation yielded the reduced probabilities $B(M1,\sigma)$ of β transitions to these states. Figure 3 shows the strength functions of Gamow–Teller β decay for ^{236}Pa and ^{238}Pa. The behavior of S_β does not change qualitatively if the parameters used in the calculation are varied in reasonable limits.

The strength functions for the nuclei ^{232}Pu, ^{244}Cm, and ^{248}Fm, which undergo electron capture, were determined[17,18] on the basis of the following assumptions. The quasiparticles are uniformly distributed over the $h_{9/2}$, $i_{13/2}$, and $f_{7/2}$ proton subshells and the $g_{9/2}$, $i_{11/2}$, and $j_{15/2}$ neutron subshells. The Hamiltonian $H = \mathcal{G}_0(\tau\tau)/2 + \mathcal{G}_1(\tau\tau)(\sigma\sigma)/2$ of the system is diagonalized on the basis of the states 1–4. Further, $\Delta_n = \Delta_p = \Delta = 0.4$ MeV, and the spin of the parent state is assumed to be I^π:

1. $p_{i_{13/2}} \to (n_{i_{11/2}} \otimes n_{i_{11/2}})_{0^+}$, $E = 0$;
2. $p_{i_{13/2}} \to (n_{i_{11/2}} \otimes n_{i_{11/2}})_{2^+}$, $E = 2\Delta_n$;
3. $p_{i_{13/2}} \to (n_{i_{11/2}} \otimes n_{i_{11/2}})_{0^+}$, $E = 2\Delta_n$;
   $\to (p_{i_{13/2}} \otimes p_{i_{13/2}})_{2^+}$;
4. $\left.\begin{matrix} p_{i_{13/2}} \\ n_{i_{11/2}} \end{matrix}\right\} \to [(p_{i_{13/2}} \otimes n_{i_{11/2}})_{1^+} \otimes (p_{i_{13/2}} \otimes n_{i_{11/2}})_{1^+}]_{0^+, 2^+}$,

$E = 2\Delta_p + 2\Delta_n$.

The main uncertainty in the position of the S_β peaks is due to the pairing energy. Allowance for deformation of the nuclei must lead to a broadening of the peaks by not more than 1 MeV.

Fission and radiative widths. The fission width Γ_f is determined by the relation

$$\Gamma_f = p(E)\,[2\pi\rho(E)]^{-1}, \tag{7}$$

where $p(E)$ is the barrier penetrability, and $\rho(E)$ is the level density. The penetrability $p(E)$ of the two-humped barrier is determined by the solutions of the Schrödinger equation for the reflected and the incident wave when the potential is given by joined parabolas that approximate the two-hump barrier (see Refs. 19 and 20). For a single-hump barrier, the penetrability is described by the classical formula[21]

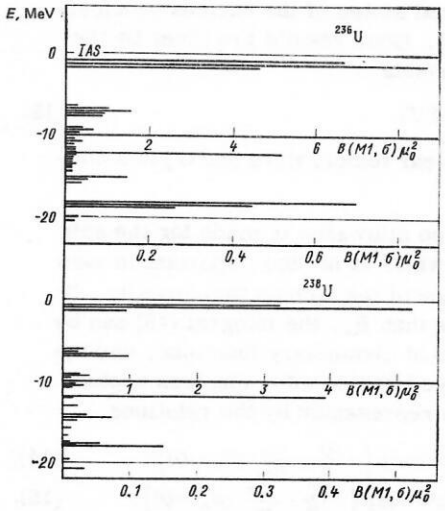

FIG. 3. Calculated Gamow–Teller strength functions S for the nuclei ^{236}U and ^{238}U.

$$p(E) = \{1 + \exp[(2\pi/\hbar\omega)(B_f - E)]\}^{-1}, \tag{8}$$

where B_f is the maximal height of the barrier, and $\hbar\omega$ is the curvature of the barrier.

It is expedient to represent the level density at low excitation energies $E < 3$ MeV by the dependence (9) obtained on the basis of the model of constant nuclear temperature[22]:

$$\rho_1(E) = T^{-1} \exp[(E - E_0)\,T^{-1}]. \tag{9}$$

At a higher excitation energy, it is more correct to describe the level density using the Fermi-gas model:

$$\rho_2(E) = A_0 \exp(2\sqrt{aE}). \tag{10}$$

The energy $E_x = U_x + C$ at which the functions $\rho_1(E)$ and $\rho_2(E)$ must be matched lies in the interval from 2.5 to 3.5 MeV. In $E_x, U_x = 2.5 + 150A^{-1}$ and $C = 26A^{-1/2}$. The nuclear temperature at mass numbers ≥ 200 is in the range from 0.30 to 0.45 MeV. The value of E_0 is small compared with the Q_β of the considered nuclei. The parameter a for deformed nuclei is related to the mass number A by $a = 0.120A$. As a rule, the width Γ_γ is calculated with allowance for only E1 transitions. If it is assumed that the transition probability satisfies the E_γ^3 rule, and we integrate over the final states, then

$$\Gamma_\gamma(E, J^\pi) = C_1 A^{2/3} D(E, J^\pi) \sum_{J_f = |J-1|}^{J+1} \int_0^E \rho(\varepsilon, J_f^\pi)\,(E-\varepsilon)^3\,d\varepsilon, \tag{11}$$

where J_f is the spin of the final state, and $C_1 = 0.002 \times 10^{-6}$ MeV^{-3}.[23]

At low excitation energies, the ratio $\Gamma_f/\Gamma_t = \Gamma_f(\Gamma_f + \Gamma_\gamma)^{-1}$ can be expressed in terms of the penetrability $P_A = 2\pi\rho\Gamma_f$ of the first barrier and the radiative penetrability $P_\gamma = 2\pi\rho\Gamma_\gamma$:

$$\Gamma_f/\Gamma_t = P_A\,(P_A + P_\gamma)^{-1}\,R; \tag{12}$$

here, R is the probability of fission from the lowest state in the second well.[24] We determine P_A in accordance with the relation (8). The function P_γ can be calculated if detailed allowance is made for the structure

of the initial and final states of the nucleus which undergoes the β decay. Good results are given by the semi-empirical formula

$$P_\gamma(E) = C_\gamma T^4 \exp(E/T), \tag{13}$$

where T is the nuclear temperature and C_γ is a constant.

In this relation, no allowance is made for the spin dependence of P_γ, which is not too important in view of the weak influence of the spin on this quantity. If Q_β is 1–2 MeV less than B_A, the integral (16) can be expressed in terms of elementary functions, and the probability of delayed fission after electron capture and β decay can be represented by the relations

$$P_{ec} = 6Ra^{-3}Q^{-3}C_\gamma^{-1}\Theta^{-4}\exp\left\{-\frac{Q}{\Theta}-\frac{2\pi}{\hbar\omega_A}(B_A-Q)\right\}; \tag{14}$$

$$P_{\beta f} = 720Ra^{-6}Q^{-6}C_\gamma^{-1}\Theta^{-4}\exp\left\{-\frac{Q}{\Theta}-\frac{2\pi}{\hbar\omega_A}(B_A-Q)\right\}. \tag{15}$$

where $a = (2\pi/\hbar\omega_A) - \Theta^{-1}$ (see Ref. 24).

The expressions (14) and (15) relate the probability of delayed fission to the height of the inner barrier B_A and the curvature $\hbar\omega_A$. It follows from them that the probability of delayed fission for the same values of the basic parameters Q_β, B_A, and $\hbar\omega_A$ is higher in the case of electron capture than for β decay. This is explained by the greater probability of population of high-lying levels in the neutron-deficient nuclei. The ratio Γ_f/Γ_n, which is needed for the calculation of P_{df} for neutron-deficient nuclei, can be calculated in accordance with the equations of Ref. 25.

The basic expression for calculating P_{df} for neutron-deficient nuclei is

$$P_{df} = \int_c^{Q_{ec}-B_k} b(E)\frac{\Gamma_f}{\Gamma_f+\Gamma_\gamma}(E)\,dE \Big/ \int_c^{Q_{ec}-B_k} b(E)\,dE, \tag{16}$$

where $b(E)$ is the probability of population of levels in the region of the excitation energy E, $\Gamma_f(E, J^\pi)$ is the fission width, and $\Gamma_\gamma(E, J^\pi)$ is the γ width, J^π denotes the spin and parity, Q_{ec} is the energy of electron capture, B_k is the binding energy of the k-th electron, and

$$b(E) = S_{ec}(E)\, f(Z, Q_{ec} - E). \tag{17}$$

Here, $f(Z, Q_{ec} - E)$ is the Fermi function. For electron capture,

$$f(Z, Q_{ec} - E) \sim (Q_{ec} - E - B_k)^2.$$

For neutron-rich nuclei, P_{df} can be calculated in accordance with

$$P_{df} = \int_c^{Q_\beta} b(E)\,\Gamma_f(E)/\Gamma_t(E)\,dE \Big/ \int_c^{Q_\beta} b(E)\,dE, \tag{18}$$

where $\Gamma_t(E) = \Gamma_f(E) + \Gamma_\gamma(E) + \Gamma_n(E)$. The Fermi function is $f(Z, Q_\beta - E) \sim (Q_\beta - E)^5$.

2. BASIC EXPERIMENTAL RESULTS

Discovery of delayed fission of neutron-deficient nuclei. Delayed fission was observed for the first time when ^{233}U was irradiated with ^{10}B and ^{11}B ions.[1] The first search experiments were specially prepared to study fissioning nuclei with large neutron deficit. The employed method made it possible to detect fission of nuclei produced with a cross section of 10^{-34}–10^{-35} cm^2. The experiments were made possible by the high intensity of the beams of accelerated heavy ions (100 μA of B^{+2} and Ne^{+4}) and strong targets, which made it possible to realize high currents. The fission fragments were detected by means of low-background solid-state track detectors with an efficiency of fission-fragment detection of 0.90 ± 0.05.

In the experiment, an inclined target and movable track detectors were used. The target was inclined at 9° to the direction of the heavy-ion beam. Thus, the energy of the beam was distributed over a large surface, which made it possible to cool the target by simple means. On the other hand, the recoil nuclei formed in the nuclear reactions were stopped in a thin surface layer of matter equal to $\lambda \sin\alpha$, where λ is the range of the ion in the material of the target, and α is the angle of inclination of the target to the direction of incidence of the heavy ions (Fig. 4). As a result, the fission fragments escaped from the matter with a very high efficiency. A screen above the target, which played the part of a Faraday cylinder, and the electric insulation of the target with a cooling circuit made it possible to measure the current of the ions reliably (see Fig. 4). After a cycle of irradiation of the target with some exposure of heavy ions, the solid-state detectors were placed above the target automatically, the time required to transport them from their chamber to the target being $\geq$10 sec. A cassette system of mounting the detectors made it possible to exchange them rapidly, which is particularly important in the case of appreciable activity of the target in the experiments, when the cross section for the production of fissioning nuclei is about 10^{-34} cm^2 and, therefore, the exposures of the accelerated particles are high.

In the first experiments using the U-300 cyclotron of multiply charged ions, the isotope ^{233}U was irradiated with ^{10}B and ^{11}B ions. The intensity of the boron ions reached about 10^{14} particle/sec. At ^{11}B energies greater than 75 MeV, fission fragments of the nuclei were detected with half-lives of minutes. The decay curve of the synthesized nuclides could be clearly divided into two exponentials corresponding to half-lives of 5 $\pm$1 sec and 2.6 $\pm$ 0.2 min. The decay of the nuclei with half-life 2.6 min was studied in detail. The influence

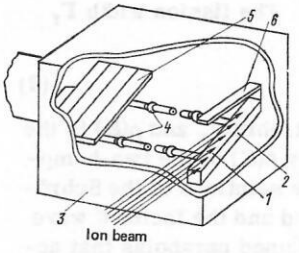

FIG. 4. Arrangement of experiment with inclined target: 1) target, 2) cooled frame, 3) casing, 4) insulators, 5) movable solid-state detectors, 6) screen.

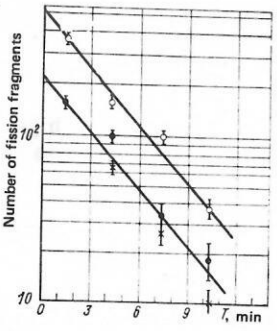

FIG. 5. Decay curves of ^{234}Am produced in the reaction ^{233}U $+^{10}$B (open circles) at $E_{^{10}B}=60$ MeV and the reaction ^{233}U$+^{11}$B (black circles) at energy $E_{^{11}B}=75$ MeV; the crosses correspond to energy $E_{^{11}B}=80$ MeV. The curves are obtained from measurements of delayed-fission fragments.

of the short-lived component was eliminated by delaying the detection of the fission fragments by 33 sec. The number of heavy ions in each irradiation cycle was 6×10^{16} ions, and the range in U was 4.5 mg/cm^2.

After detection of the effect, a measurement was made of the excitation function of the reaction leading to the formation of the nuclides with $T_{1/2}=2.6$ min. The experiments were made in a thin target, in which the maximal energy losses of the ^{11}B ions did not exceed 1 MeV. For each energy of the accelerated ions measurements were made of not only the yield of the fissioning nuclei but also their decay curves (Fig. 5). It could be deduced from the decay curves that for energies of the ^{11}B ions from 75 to 83 MeV the same fissioning nuclide with a half-life of $T_{1/2}=2.6$ min is synthesized in the ^{233}U$+^{11}$B reaction. The excitation function of the reaction is shown in Fig. 6. An estimate of the cross section for production of the fissioning isotope at the energy corresponding to its maximal yield gives 2×10^{-33} cm^2. In the case of irradiation of ^{233}U with ^{10}B ions of energy 60 MeV a fissioning product with a half-life of $T_{1/2}=2.6$ min was also detected with approximately the same production cross section. In control experiments, in which a thick ^{235}U target (4.5 mg/cm^2) was irradiated with ^{11}B ions of energy 74 and 82 MeV, fission fragments of isotopes with half-life in the minute range were not detected. Fission was also not observed in the ^{235}U$+^{10}$B and ^{232}Th$+^{10}$B reactions at an energy of the ^{10}B ions equal to 60 MeV.

Control experiments confirmed the reliability of the obtained results, since in them an external background comparable with the effect was not observed. At the same time, the form of the excitation function in the ^{233}U $+^{11}$B reaction ruled out an evaporation reaction of the type ^{233}U(^{11}B, xn), from the excitation curve of which it would be possible to identify the synthesized fissioning nuclide. The nature of the excitation function corresponded to nuclear reactions with the emission of a charged particle. The fissioning nuclei most probably arise in reactions of the type ^{233}U(^{11}B, αxn) and ^{233}U(^{10}B, αxn). Thus, an evaporation reaction could take place if boron ions are used to irradiate a target lighter than ^{233}U by an α particle, i.e., if the decay product ^{229}Th of ^{233}U decay is irradiated. However, ^{229}Th contains an admixture of the isotope ^{228}Th with half-life $T_{1/2}=1.9$ years, which produces a high background of α rays. A more suitable target is ^{230}Th, though the cross section for the production of a fissioning product when ^{230}Th is irradiated with boron ions is lower than in reactions with the light isotope ^{229}Th.

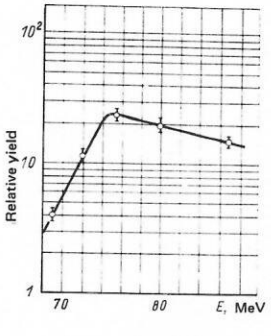

FIG. 6. Excitation function of the reaction ^{233}U(^{11}B, $\alpha6n$)^{234}Am.

The target contained the isotopes ^{230}Th and ^{232}Th. To raise the strength of the target, organic compounds were added to the active substance and the resulting mixture deposited on an aluminum substrate, after which the organic matter was burnt. The ^{230}Th thickness of the target was 250 μg/cm^2. When allowance is made for the inclination of the target, its thickness for the accelerated ions was 1.2 mg/cm^2. The energy loss of the accelerated boron ions in passing completely through the target material (with allowance for the ^{232}Th isotope, the target thickness was 2.4 mg/cm^2) was about 1.5 MeV.

When the thorium target was irradiated with accelerated ^{10}B and ^{11}B ions in the energy range from 50 to 90 MeV, fragments were detected from the fission of a nucleus that decays with a half-life of 2.6 min. The form of the excitation function corresponded to evaporation reactions with emission from the compound nucleus of six or seven neutrons. The positions of the experimentally found maxima of the excitation functions in the reactions ^{230}Th(^{10}B, $6n$)^{234}Am and ^{230}Th(^{11}B, $7n$)^{234}Am at energies 70.5 and 82 MeV of the boron ions, respectively, were equal to their calculated values when the nuclear temperature of the compound nucleus was taken equal to 1.5 MeV. Thus, the fissioning nuclei with half-life 2.6 min were identified as the nuclei of the isotope ^{234}Am.

A possible influence of the ^{232}Th present in the target material on the yield of the fissioning isotope ^{234}Am was eliminated by control experiments, in which a ^{232}Th target of thickness 5 mg/cm^2 was irradiated by 70.5-MeV and 82-MeV boron ions, corresponding to the maximal ^{234}Am yield. In these experiments, fissioning products with half-lives in the minute range were not observed. The background was due to fission of uranium contained in the glass detectors. The error introduced by the presence of the background did not exceed 5%.

The cross sections for the production of the fissioning nuclei ^{234}Am in the reactions ^{230}Th(^{10}B, $6n$)^{234}Am and ^{230}Th(^{11}B, $7n$)^{234}Am, calculated on the basis of the

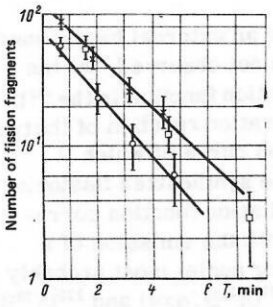

FIG. 7. Decay curves of the isotope ^{232}Am obtained by detection of the delayed-fission fragments of the reaction ^{230}Th(^{10}B, 8n)^{232}Am at different energies of the ^{10}B ions. The crosses and open squares correspond to $E_{10_B} = 88.5$ MeV, and the open circles to $E_{10_B} = 82$ MeV.

experimental data, are, respectively, $(5.7 \pm 0.5)10^{-34}$ cm^2 and $(5.4 \pm 0.5)10^{-34}$ cm^2 at the maxima of the excitation function.

At energies of the accelerated ^{10}B ions higher than 82 MeV, fissioning nuclei with half-life 1.4 min were observed. The maximum of the excitation function of this emitter was shifted by 12 MeV to higher energies. The presence of the isotope with the half-life 1.4 min was taken into account in the calculation of the ^{234}Am production cross section.

The fissioning nuclei with half-life $T_{1/2} = 1.4$ min were studied in special experiments in which the target irradiation time, the delay before the detection time of the fission fragments, and the detection time were chosen optimally to separate the half-life of 1.4 min. The total calculated detection efficiency was about 15% with allowance for the decay during the irradiation time and the delay. The decay curve is shown in Fig. 7. Figure 8 shows the excitation function of the fissioning nuclide with half-life 1.4 min with normalization of the number of fragments at each point to 2.53×10^{17} of the ^{10}B ions. The form of the excitation function, a dome with half-width 14 MeV, characterizes a nuclear reaction which proceeds through a compound nucleus with evaporation of neutrons. It was concluded from the data on the position of the maximum of the excitation function and its half-width at the 0.5 level that fission fragments of the product of the ^{230}Th(^{10}B, 8n)^{232}Am reaction were observed. Thus, the fissioning nuclide with half-life 1.4 min was identified as ^{232}Am. The cross section for the production of

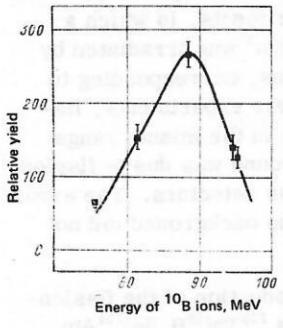

FIG. 8. Excitation function of the reaction ^{230}Th(^{10}B, 8n)^{232}Am.

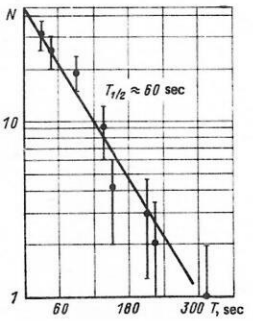

FIG. 9. Decay curve of the isotope ^{228}Np obtained by detection of delayed-fission fragments in the reaction ^{209}Bi(^{22}Ne, 3n).

^{232}Am measured in the experiments at the maximum of the excitation function at the ^{10}B energy was $(2.3 \pm 0.4)10^{-33}$ cm^2.

Analysis of the half-lives and the decay energies for e capture and α decay of the light Np isotopes suggested that delayed fission could be observed in the Np isotopes. To test this, in inclined bismuth target of effective thickness 9.5 mg/cm^2 was irradiated with accelerated ^{22}Ne ions with intensity 10^{14} ion/sec. The irradiation periods lasted 4 min, and then four detectors were placed above the irradiated material, each of them remaining in the detection regime for 1 min. In this experiment a fissioning isotope with half-life 60 ± 5 sec was observed when the target was irradiated with 110-MeV neon ions. Figure 9 shows the decay curve obtained in two independent experiments by means of solid-state detectors. The excitation function of the fissioning isotope was obtained by irradiating a thin bismuth target with ^{22}Ne ions (the range of a ^{22}Ne ion was 2.1 mg/cm^2). The background due to the fission of the impurity uranium in the detectors was determined from the number of tracks observed in the parts of the detectors shielded from the fission fragments of the products of the nuclear reaction ^{209}Bi(^{22}Ne, xn).

The form and position of the maximum of the excitation function of the nuclide with $T_{1/2} = 60$ sec (Fig. 10) corresponded to a nuclear reaction which proceeds through the formation of a compound nucleus with the evaporation of three neutrons. Production of fissioning isotopes in the ^{209}Bi(^{22}Ne, $p2n$) and ^{209}Bi(^{22}Ne, $p3n$) reactions was eliminated by control experiments in which lead was irradiated with neon. In the ^{208}Pb(^{22}Ne,

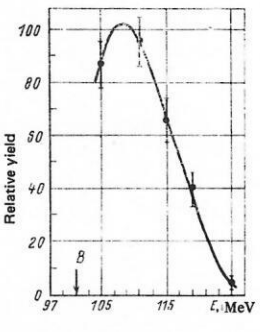

FIG. 10. Excitation function of the reaction ^{209}Bi(^{22}Ne, 3n)^{228}Np.

$4n$) and $^{208}Pb(^{22}Ne, 3n)$ reactions, fissioning products with a half-life around 1 min were not observed in a wide range of ^{22}Ne energies. Nor was fission detected when ^{209}Bi was irradiated with ^{18}O ions of energy sufficient for the reaction $^{209}Bi(^{18}O, \alpha 3n)$ to take place. The various experiments made it possible to identify the fissioning isotope with half-life 60 sec as ^{228}Np. The cross section for the production of the fissioning nuclei at the maximum of the excitation function of the $^{209}Bi(^{22}Ne, 3n)$ reaction is 4.5×10^{-34} cm^2.

Thus, by means of the heavy-ion beams the nuclei ^{228}Np, ^{232}Am, and ^{234}Am were synthesized and their daughter products ^{228}U, ^{232}Pu, and ^{234}Pu undergo fission from excited states formed after electron capture. For the neutron-deficient nuclei, the daughter products of ^{228}Np and $^{232,234}Am$, the neutron separation energy satisfies $B_n > Q_{ec}$, and, therefore, the probability of delayed fission of the identified nuclei can be calculated theoretically in accordance with Eq. (16) without allowance for the possible emission of delayed neutrons. The probability of delayed fission can be calculated in accordance with the relation (2) on the basis of the experimental data.

Delayed fission of ^{232}Am nuclei was investigated in the nuclear reactions $^{247}Np(\alpha, 9n)^{232}Am$, neptunium being irradiated with 104-MeV α particles.[26] In this reaction, fissioning nuclei with a production cross section $(5\pm1)10^{-33}$ cm^2 were observed. In the experiment, the recoil nuclei that escaped from the target of thickness 100 μg/cm^2 were stopped in a graphite film 100-μg/cm^2 thick situated 5 mm from the target. After irradiation, the collecting film was transported pneumatically to the gap between two closely spaced surface-barrier detectors 60 cm from the irradiated target. Fission fragments and α particles were detected simultaneously when the reaction products decayed. The decay curve of the fissioning nuclei, identified as ^{232}Am, is shown in Fig. 11.

Other possible nuclei were eliminated by a number of arguments. For example, if it is assumed that the observed decay is associated with the production of the nucleus ^{228}Np, then the experimental data indicate a probability of delayed fission of this nucleus several orders of magnitude higher than the values obtained in Refs. 2 and 27. If the source of the fission fragments were ^{231}Pu, its probability P_{df} would have to be about

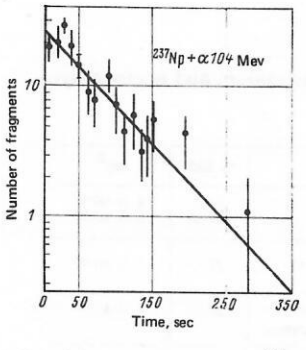

FIG. 11. Decay curve of ^{232}Am obtained by detecting delayed fission in the reaction $^{237}Np(\alpha, 9n)$.

8%. At this probability of delayed fission, the barrier parameters for this isotope are such that its calculated half-life until spontaneous fission is about 10^3 min. But this contradicts the half-lives of order 10^{10} years known for the neighboring isotopes of neptunium and plutonium. Other nuclei were ruled out by the argument that their fission fragments were not observed in the heavy-ion reactions leading to production of the ^{232}Am and ^{234}Am isotopes.[3]

Data on the α decay of the ^{232}Am isotope were obtained by measurements of the coincidences of the α particles emitted by the neighboring α emitters in the chain of ^{232}Am transformations with half-lives in the microsecond range. The ratio of the probabilities of α decay and electron capture was estimated with an accuracy of about 50%. The cross section $\sigma_{ec}=(0.4^{+1.2}_{-0.2})$ μb was calculated from the measured ^{232}Am production cross section on the basis of the yield of the α-active nuclei. A certain discrepancy observed between the ^{232}Am half-lives studied in the α-particle and heavy-ion reactions can be attributed to the low statistics and, apparently, an appreciable background in the experiments with the α-particle beams. Actually, the agreement is fairly good and lies within the limits of the experimental errors.

The further development of the study of delayed fission of neutron-deficient nuclei is associated with the study of fission in the process of electron capture of the odd–odd isotopes of beryllium, einsteinium, and mendelevium.

The isotopes ^{240}Bk, ^{242}Bk, ^{246}Es, and ^{248}Es were obtained by irradiating thick uranium and thorium targets with $^{14}_{7}N$ ions with beam intensity up to 10^{14} sec^{-1}. The active substance was deposited on an inclined target, which was irradiated on the inner orbits of the cyclotron. A polyethylene–terephthalate film was used to detect the fission fragments. After chemical processing of the film, the tracks of the fragments were counted by means of an optical microscope. In some experiments, the fission events were detected by solid-state breakdown detectors, whose principle of operation is based on the reduction of the dielectric strength of the film when a fission fragment passes through it and the breakdown of the film at this position by a voltage applied to the film.[28,29]

At nitrogen-ion energies in the range from 74 to 76 MeV, ^{248}Es and ^{242}Bk nuclei were synthesized in the reactions $^{238}U(^{14}N, 4n)^{248}Es$ and $^{232}Th(^{14}N, 4n)^{242}Bk$.

In these experiments, it was possible to detect only a few fission fragments. Despite the low statistics, the cross section for the production of ^{248}Es was estimated, and an upper limit for the probability of delayed fission of ^{242}Bk was established.

When ^{238}U and ^{232}Th were irradiated by ^{14}N ions with energy in the interval 92–94 MeV, a maximal yield of fission fragments of nuclei decaying with half-lives 8 ± 2 and 5 ± 2 min was detected. The energy interval 92–94 MeV corresponds to maxima of the excitation functions of the reactions $^{238}U(^{14}N, 6n)^{246}Es$ and $^{232}Th(^{14}N, 6n)^{240}Bk$, and the measured half-lives are equal to the

half-lives of the isotopes ^{246}Es and ^{240}Bk. These data unambiguously indicate that the fission fragments belonged to daughter products of ^{246}Es and ^{240}Bk.

Because of the small cross sections for the production of the nuclides that undergo delayed fission in the reactions considered above, it was very important to take into account possible sources of background fission fragments. Thus, when a thick target was irradiated, allowance was made for the possible background resulting from fission of the active material of the target by delayed neutrons of prompt fission fragments, hard γ rays emitted by the fragments of prompt fission, and γ rays from nuclei produced in nuclear reactions in the target substrate.

The results of the control experiments showed that the background due to γ rays and delayed neutrons of the prompt fission fragments can be eliminated by introducing a 10-min interval between the irradiation of the target by the heavy ions and the start of detection of the fragments by the detectors. The use of a pure aluminum substrate significantly reduces the flux of γ rays and, therefore, makes it possible to reduce the background which arises from the interaction of the material of the target with the γ rays generated in the substrate.

In the same experiments, it was shown that in thick U and Th targets there is a background inadmissible for study of delayed fission with half-lives of the order of tens of minutes and production cross sections around 10^{-35} cm^2. As a result, ^{244}Es and ^{248,250}Md were synthesized by collecting the recoil nuclei knocked out of a thin target and transporting them to the fission-fragment detectors.[24] The thickness of the active material of the target was in the range from 0.5 to 1.0 mg/cm^2, and the current did not exceed 5 μA.

Figure 12 shows the distribution in time of the yields of fissioning nuclei detected in the reactions ^{235}U(^{14}N, 5n) and ^{237}Np(^{12}C, 5n)^{244}Es at ion energy 82–86 MeV with half-life 37 sec of the delayed fission and in the reaction ^{243}Am(^{12}C, 5n)^{250}Md with $T_{1/2}$ = 52 sec. Comparison of the data on the yield of the fissioning nuclei and the daughter nuclei of the ^{244}Es and ^{250}Md isotopes formed after electron capture of ^{244}Cf and ^{250}Fm made it possible to estimate the cross section for the production of delayed-fission emitters.

For nuclei with $Z > 95$, a delayed-fission effect was observed with low statistics. The main statistical material was collected in a first cycle of studies to detect and investigate this phenomenon for neutron-deficient nuclei,[1-3] which is due to the relatively high cross sections for the production of the fissioning nuclei Np and Am in reactions with accelerated heavy ions.

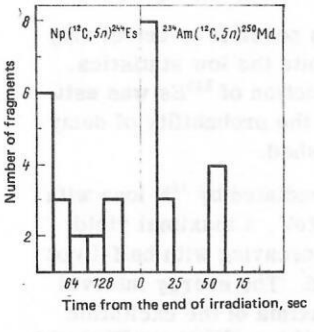

FIG. 12. Distribution in time of the fragments from the delayed fission of ^{244}Es and ^{250}Md.

This also explains why delayed fission of the ^{232,234}Am isotopes has been observed in different nuclear reactions in several laboratories. The characteristics obtained in the delayed-fission experiments agree well.

Delayed fission of neutron-rich nuclei. The possibility of observing delayed fission of neutron-rich nuclei was first pointed out in Ref. 30. The first experimental results on the delayed fission of neutron-rich nuclei were obtained by synthesizing the ^{238}Pa isotope.[31] Subsequently, delayed fission of the ^{234,236,238}Pa isotopes was studied.[32]

The decay characteristics of these isotopes,[32] the synthesis reactions for them, the production cross sections, the energies, and the intensities of the irradiating particles are given in Table I.

The cross sections of the reactions with deuterons and neutrons of energy 14.7 MeV were studied earlier.[33] For the synthesis of ^{238}Pa in a neutron flux with neutron energies from 8 to 20 MeV obtained by irradiating a thick beryllium target with deuterons, the mean cross section of the ^{238}U(n,p) reaction was estimated from the neutron spectrum, the excitation function of the (n,p) reaction, and the known cross section of the reaction at 14.7 MeV. For other reactions, the cross sections were determined from the yield of γ lines in the decay process of the ^{234,236}Pa isotopes. Because neutrons, γ rays, α particles, and deuterons have a high penetrating capacity, thick targets were used. The particle flux was immediately incident on 20 films of U or Th (each of thickness 100 mg/cm^2). The films were arranged at intervals of 4 mm, and after that irradiation fragment detectors were introduced into the gaps between them. Successive replacement of them in time made it possible to measure the decay curve of the fragment activity. In the case of irradiation of uranium with neutrons, the thin films of the matter were moved next to each other. After the irradiation cycle, the films were moved apart and dielectric detectors of polyethylene–terephthalate films were inserted in the resulting gaps.

TABLE I. Characteristics of protactinium and nuclear synthesis reactions.

Isotope	I^π	$T_{1/2}$, min	Reaction	E, MeV	σ, cm^2
^{238}Pa	3$^-$	2.3	^{238}U (n, p)	14.7 8—20	$1.5\cdot10^{-27}$ $3.0\cdot10^{-27}$
^{236}Pa	1$^-$	9.1	^{238}U (γ, n, p)	27.0	$1.0\cdot10^{-27}$
^{234}Pa	4$^-$ 0$^-$	6.7 1.2	^{232}Th (α, pn) Chemical separation	36.0 —	$3.0\cdot10^{-27}$ —
^{236}Pa	1$^-$	9.1	^{238}U (d, α)	18.0	$1.0\cdot10^{-28}$

Despite the use of the thick targets, the number of detected fissioning nuclei was low, which made it necessary to undertake a careful analysis of the possible sources of the background and adopt measures to eliminate them. As a result of the adopted measures, the observed number of tracks of fission fragments produced in the investigated nuclear reactions in the delayed-fission process exceeded the background level in all the experiments except the one with the 14.7-MeV neutrons.

The small number of detected fragments and the relatively high level of the background permitted only an approximate determination of the half-lives of the observed activities. The obtained data do not contradict the known half-lives of ^{238}Pa and ^{236}Pa. Analysis of the nuclear characteristics of the isotopes formed in the reactions studied in parallel showed that none of the possible products of these reactions could be the source of the fragment activity, this being due to the very short lifetime of the spontaneously fissioning isomers (~10^{-6} sec), on the one hand, and the long half-lives until spontaneous fission from the ground state, on the other. Delayed fission of the isotope ^{234}Pa was not detected.

The number of detected tracks of fission fragments was normalized in the experiments relative to the yield of prompt-fission fragments. This last yield was determined from the γ radiation of the fragment ^{140}Ba. The obtained ratio made it possible to calculate the cross section σ^f for production of fragment activity and the probability $P_{df}=\sigma^f/\sigma$ of delayed fission.

Delayed fission of ^{236}Pa was studied in the ^{238}U(p, $2pn$)^{236}Pa reaction.[34] A beam of 1-GeV protons was used to irradiate a target made of uranyl nitran and containing 5 g of U. The time of single irradiation was 7 min. After chemical separation of the Pa isotopes from the irradiated material of the target, which lasted 6 min, the fraction containing the Pa isotopes, but purified of uranium, was placed between mica fission-fragment detectors. Simultaneously with the detection of the fission fragments, the γ spectrum of the Pa isotopes was measured by means of a GeLi detector. The total number of synthesized ^{236}Pa atoms was determined from the decay of the most intense ^{236}Pa line with energy $E=642$ keV. The contribution to the intensity of this γ line of ^{236}Pa due to the impurity isotopes ^{131}Sb, ^{101}Mo, and ^{118}In was not more than 20%.

Altogether nine fission events were observed in the experiments for a total of 7.2×10^9 decays of the ^{236}Pa isotope. Thus, the probability of delayed fission of ^{236}Pa in experiments with 1-GeV protons is of order 10^{-9}.

The obtained experimental data on the delayed fission of the Pa isotopes are given in Table II. Because of the low statistics of the events and the appreciable influence of the background that arises in the process of fission of U by delayed neutrons and by the γ radiation of the fission fragments, the data are approximate in nature. Despite this, the data yielded information about the delayed-fission mechanism, in particular,

TABLE II. Experimental data on the delayed fission of Pa isotopes.

β transition	Q, MeV	Reaction	E, Mev	σ^f, cm^2	P_{df}
^{238}Pa → ^{238}U	4.0	(n, p) (n, p)	14.7 8—20	10^{-33} $5\cdot10^{-35}$	$6\cdot10^{-7}$ $1.0\cdot10^{-8}$
^{236}Pa → ^{236}U	3.1	(γ, np) (d, α) (p, $2pn$)	27 18 1000	10^{-36} $3\cdot10^{-36}$ —	10^{-9} $3\cdot10^{-10}$ 10^{-9}
^{234}Pa → ^{234}U ^{234}Pa → ^{234}U	2.2 2.3	(α, np) Chemical separation	36 —	$<10^{-8}$ —	$<3\cdot10^{-12}$ $<10^{-12}$

approximate values of the probabilities of delayed fission or upper bounds on these probabilities for the Pa isotopes.

Thus, in the extensive region in which delayed fission of neutron-rich nuclei should be observed, only the Pa isotopes with comparatively small neutron excess have been studied experimentally. The small excess is the reason for the low statistics of the observed events.

The impossibility of investigating neutron-rich nuclei with $Q_\beta > B_f$ is explained by the absence at the present time of methods of synthesizing nuclides with large neutron excess and accessible for direct measurement of their nuclear transformations. The neutron-rich isotopes produced in underground thermonuclear explosions decay in a time much too short for their extraction.

It will be possible to obtain experimental information on the delayed fission of neutron-rich nuclei, which play an important part in the process of nucleosynthesis in the Universe and in the pulsed neutron fluxes from thermonuclear explosions, when new experimental methods and means have been created (see, for example, Sec. 4).

3. DETERMINATION OF PARAMETERS OF FISSION BARRIERS FROM EXPERIMENTAL DATA ON DELAYED FISSION

In recent years, significant progress has been achieved in experimental and theoretical investigations of the fission barriers of nuclei, which represent the main characteristic of the fission process and determine the stability of the heaviest nuclei, including the possible existence of superheavy elements.

Currently, the main bulk of the existing experimental data on fission barriers refers to the region $90 \lesssim Z \lesssim 98$, $140 \lesssim N \lesssim 156$, which is situated in the β-stability valley. The most detailed information is obtained primarily in reactions of the type (d,pf), (t,pf), $(^3\mathrm{He},df)$, etc., and also in (n,f) reactions.

The basis of modern ideas about fission barriers of heavy nuclei and their dependence on N and Z is the concept of the deep influence of shell effects on the deformation energy; according to this conception, the nuclear shells do not disappear when deformation occurs but are only modified. The most fruitful theoretical method of investigating fission barriers is the

macroscopic–microscopic approach to the determination of the nuclear deformation energy developed in Ref. 35 and especially Refs. 36 and 37. In this method, the major part of the total energy of a nucleus is calculated macroscopically on the basis of the liquid-drop model or generalizations of it, and the contribution of the internal structure effects is taken into account by the shell correction and a pairing correction. Thus,

$$E(q, N, Z) = \tilde{E}(q, N, Z) + \delta E(q, N, Z),$$

where q is the set of deformation parameters that determine the shape of the nucleus, $E(q,N,Z)$ is the macroscopic part of the total energy describing the smooth variations of E, and $\delta E(q,N,Z)$ is the microscopic correction, which reflects the local fluctuations of E and is calculated by Strutinskiĭ's method using some single-particle potential for the deformed shapes of the nucleus. The investigation of the extrema of the surface $E(q,N,Z)$ leads to the determination of the fission barriers.

Within the framework of the basic idea, there are variants of the method, which differ in the parametrization q of the shape of the nuclear surface, the particular model used to calculate the smooth part of E, and the nature of the single-particle potential for calculating the microscopic correction δE.

Despite this, the variants of the method lead to very similar results for nuclei in the β-stability valley. It is therefore difficult to give preference to any particular variant of the method on the basis of the existing experimental data for nuclei in the β-stability valley.

Far from the line of β stability, the predictions of the different variants differ not only quantiatively but even qualitatively. For example, the liquid-drop model in the variant of Myers and Swiatecki[35] and the "droplet" model give directly opposite tendencies for the variation of the macroscopic part of the barrier as a function of $I=(N-Z)/A$, which leads to large discrepancies for nuclei far from the line of β stability. Therefore, study of the fission barriers of nuclei far from the line of β stability can be used to judge the applicability of a particular model and in this connection is very valuable. However, the barrier parameters of such nuclei cannot be determined by the ordinary experimental methods, which involve induced-fission reactions at low excitation energies[23,38] and reactions in which spontaneously fissioning isomers are produced. The problem is the absence of suitable targets or spontaneously fissioning isomers in the investigated region of nuclei.

The investigation of delayed fission offers a unique possibility of obtaining data on the fission barriers of nuclei very far from the line of β stability. The already existing experimental means make it possible to plan experiments to study neutron-deficient nuclei which are removed by 15–20 units in N from the line of β stability.[40] Parameters of the fission barriers have already been obtained for some neutron-deficient nuclei from experimental data on delayed fission. The parameters of the barriers of the Pu nuclei were calculated from the probabilities of delayed fission of the isotopes ^{232}Am and ^{234}Am.[26,40]

As a rule, the two-hump fission barrier calculated by Strutinskiĭ's method is approximated by a curve consisting of joined sections of parabolas in order to determine the penetrability of the barrier and the transitions between the levels in its potential wells (and also to make other calculations). In this case, the shape of the barrier is uniquely determined by five parameters: the heights of the inner and outer barriers, E_A and E_B, their curvatures $\hbar\omega_A$ and $\hbar\omega_B$, and the energy of the intervening minimum E_{II} relative to the ground state.

The probability of delayed fission can be represented in the form

$$P_{df} = f(Q_{ec}, E_A, E_B, \hbar\omega_A, \hbar\omega_B) \qquad (19)$$

[see Eqs. (16) and (18)]. To determine the barrier heights E_A of the neutron-deficient Pu nuclei from the values of P_{df}, two families of curves $E_A = F(Q_{ec})$ were constructed for the interval of P_{df} from 10^{-1} to 10^{-7} sec with fixed values of E_B equal to 4.0 MeV (continuous curve) and 4.5 MeV (broken curve). For both families, $\hbar\omega_A = 0.9$ MeV and $\hbar\omega_B = 0.6$ MeV. The dependence (17) was used under the assumption that $S_{ec} = \text{const}$ if $E > C$ and $S_{ec} = 0$ if $E < C$. If the heights E_A and E_B of the fission barriers measured in prompt-fission reactions and in the decay of spontaneously fissioning isomers are extrapolated to the region of the neutron-deficient isotopes of Pu, then $E_A > E_B$ (Fig. 13). From this extrapolation, the height of the outer barrier E_B of the isotope ^{232}Pu is less than 4.2 MeV. Because Q_{ec} for the nucleus ^{232}Am is greater than the second barrier of ^{232}Pu by at least 0.8 MeV, the probability of delayed fission for the adopted form of S_{ec} is primarily determined by E_A. In the curves of Fig. 13, this is expressed in the fact that E_A is virtually independent of the choice of E_B in the region of 4.2 MeV, and it can be found from the graph $E_A = f(Q_{ec})$. As a result, the inner barrier E_A of ^{232}Pu is 5.3 ± 0.4 MeV.

In Ref. 26, it is noted that a possible structure of S_{ec} occupying a band of width 1 MeV with an amplitude three orders higher than S_{ec} in the region $E > C$ could

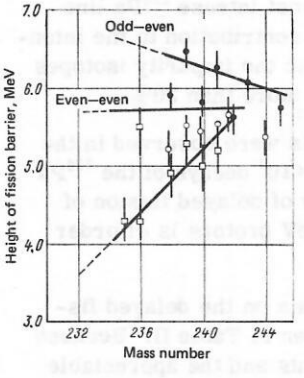

FIG. 13. Fission-barrier heights E_A and E_B of plutonium obtained from data on the probabilities of prompt fission and data on fissioning isomers. The black circles (E_A) and the open circles (E_B) correspond to prompt fission; the black squares (E_A) and open squares (E_B), to fissioning isomers.

change E_A by ±0.6 MeV. This emphasizes the comparatively weak influence of S_{ec} on the obtained result.

The value $Q_{ec} = 4.1$ MeV for the nucleus ^{234}Am is of the same order as the extrapolated value of the outer barrier, which is in the region $E_B < 4.5$ MeV. The height of the inner barrier of the isotope ^{234}Pu is much more sensitive to the choice of a particular value of E_B than is the case for ^{232}Pu.

The height E_A of the inner barrier, calculated from the measured probability of delayed fission, takes the values 6.0 and 5.5 MeV with accuracy ±0.4 MeV if E_B is taken equal to 4.0 and 4.5 MeV, respectively.

The inner and outer fission barriers of the Th, U, Pu, and Cm isotopes are given as functions of the number of neutrons in Fig. 14. For comparison, we give the theoretically calculated static fission barriers with different single-particle potentials.[42,43] The heights of the inner barriers are lowered when allowance is made for γ deformations,[44] but these deformations do not play a part for neutron-deficient nuclei. In all the theoretical calculations, the outer barriers do not differ from the experimental ones. In contrast, the inner barriers do not agree with the experimentally determined barriers, and are lower, sometimes by about 3 MeV.

The main conclusion is that the measurements of P_{df} for the nuclei ^{232,234}Pu and the values of E_A calculated on their basis indicate the same situation for the neutron-deficient isotopes of Pu as in the region of Th, for which the theoretical calculation of the height of the outer barrier for the Th isotopes gives for them values 2–3 MeV higher than for the inner barrier, while the experimentally obtained E_A and E_B are virtually equal.

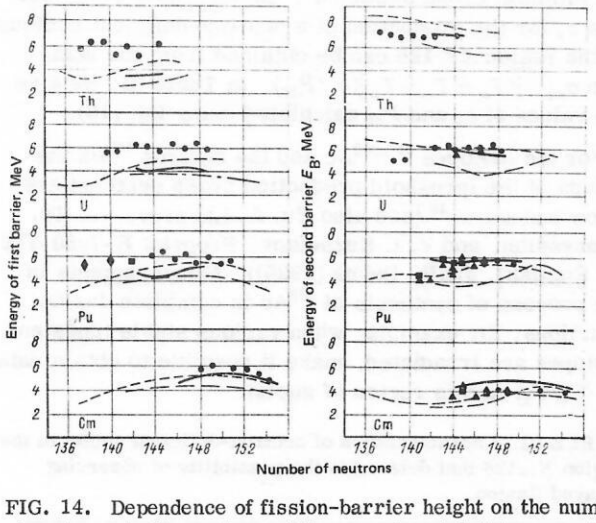

FIG. 14. Dependence of fission-barrier height on the number of neutrons in the nucleus. The experimental data were obtained in direct reactions (open circles), from the excitation functions of fissioning isomers (open squares) and their half-lives (open triangles), and from delayed fission (open diamonds). The theoretical data are based on calculations of the barriers by the shell-correction method with different single-particle potentials (broken curve for harmonic oscillator potential, and chain curve for a potential of convolution type.

As follows from the above, the extraction of information about the shape of the fission barrier from the measured value of P_{df} leads to some uncertainties because of the complicated dependence of P_{df} on the barrier parameters $E_A, E_B, E_{II}, \hbar\omega_A, \hbar\omega_B$. Additional inaccuracies are associated with the choice of the level-density distribution of the daughter nucleus and the calculation of the transition matrix elements. To eliminate these difficulties when determining the barrier parameters, it is necessary to use measurements of the delayed-fission probabilities of the neighboring odd–odd isotopes.[24] In this case, the barrier parameters are not subject to rapid changes in the even–even daughter nuclei. Using the dependences (14) or (15), it is possible to determine the E_A and $\hbar\omega_A$ averaged for the given group of even–even isotopes. The experimental data and the delayed-fission probabilities obtained on their basis for the isotopes ^{240}Bk, ^{242}Bk, ^{244}Es, ^{246}Es, ^{248}Es, ^{248}Md, and ^{250}Md (Ref. 24) were compared with the values obtained from the theoretical calculation. The dependence of P_{df} on the energy Q_{ec} was calculated in accordance with Eq. (14) when $R = 1$ and $\hbar\omega_A = 0.9$ MeV and the height of the inner barrier E_A is in the interval 5.6–6.1 MeV [see (14)]. These values of the fission-barrier parameters for the neutron-deficient nuclei listed above ensure satisfactory agreement between the calculations and the experimental data. If the measurements of P_{df} have an accuracy of 50%, the barrier heights E_A of the neutron-deficient isotopes in the region of atomic numbers 97–99 lie in the interval 5.7–6.0 MeV. Therefore, the calculation of the barrier heights from the probability P_{df} obtained from experimental data for heavy nuclei with fissility parameter Z^2/A in the interval 38–40 leads to values of E_A in the neighborhood of 6 MeV. This agrees with the situation in the region of smaller Z^2/A (34–38), where one observes a discrepancy between the measured fission thresholds and their calculated values obtained on the basis of the liquid-drop model.

With increasing Z^2/A, the fission barriers determined as a result of delayed-fission experiments decrease much more slowly than indicated by liquid-drop calculations.

A theoretical calculation was made of the delayed-fission probabilities of neutron-deficient nuclei when the strength function S_{ec} was calculated by the microscopic method of Ref. 17 and the fission barriers were determined by Strutinskiĭ's method. It was assumed that the strength function has a peak which can be represented by a Gaussian function with width 1 MeV at the level of half the maximal value.[45,46] The maximum of the S_{ec} peak is situated at an excitation energy in the neighborhood of the center of gravity of the states $0^+, 2^+$ (Fig. 15). The ratio of the maximal value of S_{ec} to its constant component was taken equal to 100. The fission probability was calculated using a parametrization corresponding to only partial overlapping of the states of the first and second potential wells.[47] As in Ref. 26, the curvature of the barriers was taken equal to 0.9 and 0.6 MeV for the inner and outer barriers, respectively. This approach to the theoretical calculation of P_{df} made it possible to reconcile the barrier heights

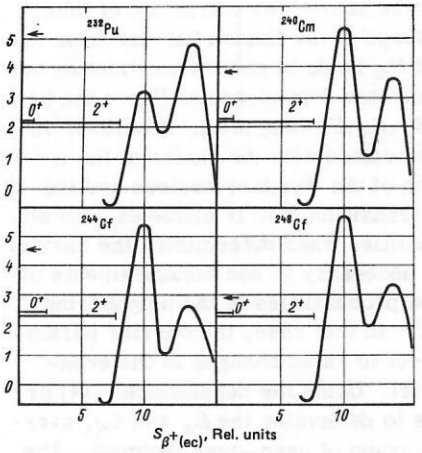

FIG. 15. Strength functions calculated for neutron-deficient nuclei by the "microscopic" method. The arrows show the energies Q_{ec}.

calculated by Strutinskiĭ's method and the experimental data on delayed fission.

For comparison of the results of calculation of the inner barrier E_A obtained under the assumption S_{ec} = const, $E > C$, and $S_{ec} = 0$, when $E < C$,[26] the height of the outer barrier was taken to be 4.2 MeV. The value $E_B = 4.2$ MeV is in good agreement with the calculation of the barrier parameters by Strutinskiĭ's method, which makes it possible to determine E_B with an accuracy of ±1 MeV, as well as with the experimental data.[24,26] Then a determination was made of the height of the inner barrier E_A when the standard deviation σ of the Gaussian function representing the S_{ec} peak had different values (Fig. 16). The ratio of the area bounded by the curve of the S_{ec} resonance structure to the area of the smooth part of S_{ec} was also varied. It was found that if σ is taken equal to the values obtained from the delayed-neutron experiments,[45,46] then for a reasonable position of the S_{ec} maximum in the Q_{ec} window the barrier E_A is in the interval 4.0–4.5 MeV, i.e., in the region predicted by the Strutinskiĭ calculation. Thus, the conclusion drawn earlier in Ref. 26 to the effect that the thorium anomaly extends to the neutron-deficient Pu nuclei must be confirmed by a detailed investigation of the structure of the strength function of the neutron-deficient nuclei.

The synthesis of neutron-deficient nuclei with $N < 126$

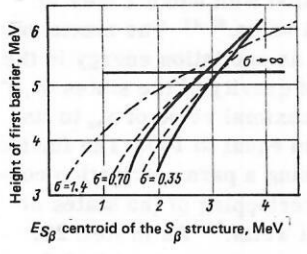

FIG. 16. Calculated heights E_A of the first barrier corresponding to $P_{df} = 1.3 \times 10^{-2}$ for different positions of the centroid E_{S_β} of the single-particle structure of the β-decay strength function. A Gaussian function is used to describe the structure.

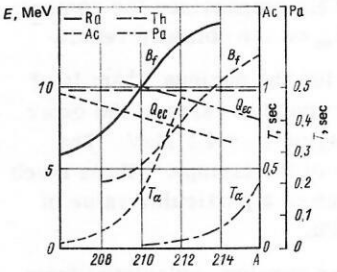

FIG. 17. Dependence of the periods T_α and T_{ec} and the energy Q_{ec} for Ac and Pa nuclei with even mass numbers and the barrier heights of the even–even Ra and Th isotopes on the number of neutrons in the region of proton-rich nuclei.

in heavy-ion reactions offers a remarkable possibility for investigating the barriers of nuclei which are 15–20 units in N from the β-stability line.

For heavy elements with Z from 81 to 99 and decreasing number of neutrons in the nucleus, the α-decay energy Q_α drops sharply when the $N = 126$ shell is crossed, and then increases fairly slowly with further increase in the neutron deficit, so that in the region adjoining $N = 126$ there are odd–odd Ac, Pa, and Np nuclei for which the ratio $T_\alpha(T_\alpha + T_{ec})^{-1}$ is not too small and the energy Q_{ec} already exceeds the height of the fission barriers of the even–even daughter nuclei.

The dependences of T_α, T_{ec}, and Q_{ec} on the number of neutrons for the Ac and Pa nuclei with even A are shown in Fig. 17, in which we also give the barrier heights of the even–even daughter nuclei calculated by extrapolating the experimental data. The currently available experimental means and the background conditions which arise in the process of synthesis of isotopes which undergo fission make it possible to detect fission fragments of nuclei for which the production cross section is 10^{-35} cm^2.[24,32] If 10^{-35} cm^2 is taken as the minimal cross section σ^f, the threshold cross section σ_n for the production of a neutron-deficient nucleus in the region $Z < 126$ can be obtained from the relation $\sigma_{xn} = [(T_\alpha + T_{ec})/T_\alpha](\sigma^f/P_{df})$. In Table III, we give the values of σ_n and P_{df} calculated using Eq. (16).

For the isotopes ^{206,208}Ac and the nucleus ^{210}Pa the values of the threshold production cross sections are a few nanobarns[48] {see also Yu. A. Lasarev, Yu. Ts. Oganessian, and V. I. Kuznetsov, Preprint E-7-80-719 [in English], JINR, Dubna (1980)}. Measurements in the process of synthesis of ^{208}Ac in complete-fusion reactions, for example, when various stable tungsten isotopes are irradiated, make it possible to obtain data on $\langle \Gamma_f/\Gamma_t \rangle$ in this region of nuclei.

TABLE III. Characteristics of neutron-deficient nuclei in the region $N < 126$ that determine the possibility of observing delayed fission.

Initial nucleus	Q_{ec}, MeV	$T_\alpha/(T_\alpha+T_{ec})$	Daughter nucleus	B_f, MeV	P_{df}	σ^f/σ	σ_n, cm^2
^{206}Ac	9.6	$3\cdot10^{-2}$	^{205}Pa	5.8	0.12	$3.6\cdot10^{-3}$	$2.8\cdot10^{-33}$
^{208}Ac	8.9	10^{-1}	^{208}Pa	7.0	0.02	$2.0\cdot10^{-3}$	$5.0\cdot10^{-33}$
^{210}Pa	10.0	10^{-2}	^{210}Th	5.1	0.20	$2.0\cdot10^{-3}$	$5.0\cdot10^{-23}$
^{212}Pa	9.3	$2\cdot10^{-2}$	^{210}Th	8.0	0.005	$0.1\cdot10^{-3}$	$1.0\cdot10^{-31}$

4. THE ROLE OF DELAYED FISSION IN THE PRODUCTION OF HEAVY ELEMENTS IN PULSED NEUTRON FLUXES

Considerable efforts have been directed toward the study of synthesis of heavy elements in pulsed neutron fluxes with high exposure ($>10^{24}$ neutron/cm^2). In the thermonuclear explosion Mike, the exposure *nvt* was about 2.0×10^{24} neutron/cm^2. Approximately the same neutron exposure was achieved in 1962 in the underground explosion Anacostia. In the underground explosions Par and Barbel in 1964 and Cyclamen in 1966 the exposures reached 4.5×10^{24} and 1.2×10^{25} neutron/cm^2, respectively.[49] In the experiment HUTCH in 1969, an exposure 4.5×10^{25} neutron/cm^2 was achieved.[50]

The duration of the neutron pulse from a thermonuclear explosion is about 10^{-6} sec. During the same time, a multiple sequence of neutron capture by target nuclei occurs. Thus, the total time of neutron capture was much less than the half-lives until β decay of the neutron-rich nuclei, which is 1 sec in order of magnitude. Therefore, the nuclear transformations in a neutron pulse from a thermonuclear explosion can be divided into two stages: the production of neutron-rich isotopes with different mass numbers A as a result of successive capture by the target nuclei, and the formation of heavy β-stable elements by successive β transformations of the produced neutron-rich nuclei.

As a rule, natural uranium targets were irradiated in the neutron pulses, but in some cases Th and even ^{243}Am was used. When the thermonuclear reaction ends after the neutron irradiation of ^{238}U, heavy U isotopes are formed up to $^{238+m}$U, where m is the maximal number of neutrons captured by the initial ^{238}U nuclei for the exposure *nvt* achieved in the experiment.

In the sequences of β transformations of the heavy isotopes, an important part is played by delayed processes, i.e., the emission of neutrons and fission after β decay. The influence of these processes on the yields of the isotopes of the heavy elements can be established by theoretical calculation. It is assumed that the nuclei undergo β decay from the ground state. The probability of population of a level of the daughter nucleus $(Z+1,A)$ with excitation energy E^* after β decay of the nucleus (Z,A) is determined by the strength function $S_\beta(E)$ and the Fermi function $f(Z,A,Q-E^*)$. From the excited state, the nucleus may undergo fission or emit a γ ray or a neutron. The widths Γ_f, Γ_γ, and Γ_n of these processes (see the Introduction) depend in a complicated manner on the properties of the nuclei which undergo the transformations, which includes the fission-barrier parameters of the daughter nucleus $(Z+1,A)$. At excitation energies comparable with the fission-barrier heights of the daughter nuclei and the neutron separation energy—and it is at such or higher energies that delayed processes occur—simplified methods of calculation can be used. Then the fission barrier can be characterized by a single parameter, the reduced height B_f^n, which is related to the maximal height $B_f = B^n - \delta$, where δ takes into account the penetrability of the barrier due to the tunneling effect. The value of δ lies in the range from 1 to 0.8 MeV.[51]

Such an approach is justified by the fact that the important excitation energies for the calculation of the yield of β-stable isotopes satisfy $E^* > B_f$, for which the structure of the fission barrier of the excited nucleus plays a comparatively small part. One can sometimes find the comment that the result of several successive β decays is not very sensitive to the fission dynamics of an individual nucleus, but this is not entirely correct,[51] since in the presence of competition between the emission of delayed neutrons and delayed fission the yield of heavy nuclei may depend strongly on the particular characteristics of one nucleus.[40]

In the model adopted to calculate the yields of the isotopes produced in a neutron pulse, Γ_f, Γ_γ, and Γ_n are functions of $E^*, B_f, B_f^n, B_n, \rho_n$, and ρ_f, where ρ_n is the level density of the daughter nucleus $(Z+1, A-1)$ produced by the emission of a delayed neutron by the excited parent nucleus, and ρ_f is the level density of the nucleus $(Z+1,A)$ above its fission barrier. The nuclear level density is used in calculations only when the excitation energy E^* exceeds the neutron separation energy B_n and simultaneously the barrier height B_f.

Depending on the relationships between B_n, B_f, and B_f^n, three cases are distinguished:

1. $B_n < B_f^n$.

If $B_f < E^*$, then delayed fission and the emission of delayed neutrons are competing processes. In the other two variants, delayed fission plays virtually no role in the transformation of the heavy nucleus: If the excitation energy satisfies the condition $E^* < B_n$, then $\Gamma_n = 0$; Γ_f is negligibly small compared with Γ_γ and, therefore, the nucleus is de-excited by a radiative process, which results in formation of the nucleus $(Z+1,A)$. If the excitation energy lies between B_n and B_f, then $\Gamma_f = 0, \Gamma_\gamma = 0, \Gamma_n = 1$ and the nucleus $(Z+1, A-1)$ is formed.

2. $B_f^n < B_n < B_f$.

If $B_f^n < E^* < B_n$, the nucleus undergoes fission, since $\Gamma_f/\Gamma_t = 1$; if $B_f < E^*$, fission and neutron emission are competing processes; if $E^* < B_f^n$, the daughter nucleus $(Z+1,A)$ is formed; if $B_n < E^* < B_f$, the reaction product is the nucleus $(Z+1, A-1)$ (Fig. 18).

3. $B_f < B_n$.

When $B_f^n < E^* < B_n$ and $\Gamma_f/\Gamma_t = 1$, fission occurs; when $\Gamma_f/\Gamma_t = 1$ and $B_n < E^*$, delayed fission and neutron emission are competing processes (see Fig. 18).

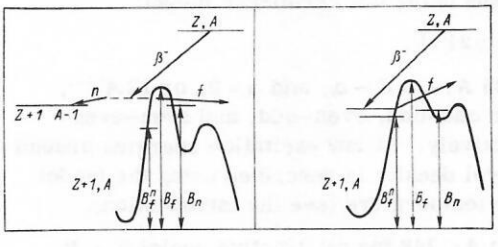

FIG. 18. Variants of delayed fission of neutron-rich nuclei.

When $E^* < B_f^n$, the nucleus $(Z+1, A)$ is formed. In the calculation of the decay probability, the width is normalized such that $\Gamma_t = \Gamma_f + \Gamma_\gamma + \Gamma_n = 1$. Thus, the functions $S_\beta, f(Z, Q-E^*)$, Γ_γ, and Γ_n make it possible to calculate the losses of heavy isotopes due to delayed fission and also the influence of the emission of delayed neutrons on the isotopic composition of the heavy β-stable elements obtained in neutron pulses.

It should be noted that for neutron-rich nuclei of heavy elements the energy Q_β may reach values large enough for E^* to be in principle sufficient for the emission of several neutrons. However, processes of the type $\beta^-, 2n$ and β^-, nf do not play a significant part at the exposures currently achieved in thermonuclear explosions. It is only when $nvt > 10^{26}$ neutron/cm^2 that they must be taken into account.

To calculate the energies Q_β and B_n, which determine the decay process, one can use different mass formulas, taking those most suitable for the specific nuclei with large neutron excess. Thus, for the considered problem the mass formula given in Ref. 52 is regarded as satisfactory; in it, the mass of a heavy deformed nucleus is a function of not only Z and A but also the deformation parameter β, which is determined by extrapolating the deformations of the studied nuclei to the region of heavy neutron-rich nuclei with allowance for the existence of the proton and neutron shells at $Z = 114$ and $N = 184$.

The fission barriers of the neutron-rich nuclei in the sequence of transformations of the products of multiple neutron capture by nuclei of a heavy target are calculated by Strutinskiĭ's macroscopic–microscopic method. The barrier parameters of the even–even nuclei in the β-decay chain obtained by calculation are known (see, for example, Ref. 53). The barriers of the odd–odd and even–odd nuclei are obtained by interpolating the barriers of the even–even nuclei with allowance for the specialization energy (0.70 MeV for the barrier height of an even–odd nucleus and 0.80–1.0 MeV for an odd–odd nucleus).

In a first approximation, the strength function of neutron-rich nuclei can be assumed proportional to the level density, since its maximum corresponding to the energy of the isobar-analog state of heavy nuclei lies in the region of 20 MeV, and on the "tail" of S_β the matrix element changes weakly and can be assumed to be effectively constant at energies below 7 MeV. However, one must allow for an influence of S_β structure at low energies.[16]

It is expedient to represent the level density of the daughter nucleus using the Fermi-gas model:

$$\rho(E) = C/U^2 \exp 2\sqrt{aU},$$

where $a = 0.125$ A, $U = E - \Delta$, and $\Delta = 0$, or $12A^{-1/2}$, or $24A^{-1/2}$ for odd–odd, even–odd, and even–even nuclei, respectively. At low excitation energies around 1 MeV, the level density is described using the model with a nuclear temperature (see the Introduction).

In the region $A < 248$ for all β-active nuclei $Q_\beta < B_f$ and $Q_\beta < B_n$ if $Z \geq 92$, and, therefore, delayed processes have virtually no effect on the yield and isotopic composition of the products synthesized in neutron pulses. The position changes from mass number $A \geq 250$. In this region, Q_β for nuclei at several units of N from the β-stability line satisfies the condition $Q_\beta < B_f, Q_\beta > B_n$. As a result, the probabilities of delayed fission and emission of delayed neutrons are fairly high and the yield of nuclei with mass number $A > 250$ depends on the delayed processes.

The greatest fission losses after β decay occur for nuclei with even mass number A. This is explained by the conditions which favor delayed fission in the process of the β decay of odd–odd nuclei. A common feature of the experiments to obtain heavy transuranium elements in neutron pulses from thermonuclear explosions is the so-called *inversion of the even–odd effect* in the isotope-yield curve. This effect is as follows. If one plots separately the yield curves of products synthesized in a thermonuclear explosion with even and odd A, the first curve initially lies above the yield curve of the nuclei with odd A beginning from some A (in the Barbel and Cyclamen experiments, in the region $A \approx 243$–249). At large A the effect is inverted, and the yield curve of nuclides with odd A drops below the even-A curve (Fig. 19) when $A > 252$. The inversion effect was also clearly observed in the Par experiment.

Various suggestions have been made to explain the effect. For example, it was assumed[54] that at the initial time of the thermonuclear process Np isotopes are accumulated as a result of $(d,n), (d,2n)$ reactions, etc. The neptunium successively captures neutrons and as a result the yield of isotopes with odd A increases in the neptunium chain by several orders compared with the uranium chain, this being due to the high cross sections of neutron capture by odd–odd nuclei. In addition, a high yield of isotopes from a small amount of ^{237}Np is explained by the circumstance that in a chain which begins with an odd-A nucleus odd–odd and odd–even nuclei alternate, whereas in a chain initiated by an even–even nucleus odd–even and even–even nuclei are formed. In the latter case, spontaneous fission is more probable, so that there is a lower yield in a chain with odd Z.[55] Although such a hypothesis appeared rather artificial, it was tested experimentally, and

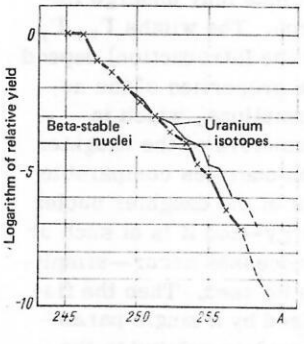

FIG. 19. Yield of uranium isotopes in the neutron flux of a thermonuclear explosion calculated on the basis of experimental data on the yield of β-stable nuclei. The inversion of the even–odd effect can be clearly seen in the region $A = 250$.

^{243}Am target material was used in the Cyclamen experiment. Analysis of the products of the thermonuclear explosion led to the conclusion that exposure of an Am target in the neutron pulse of a thermonuclear explosion does not increase the yield of isotopes of elements with $Z > 96$.

On the other hand, allowance for delayed fission in the β decay of neutron-rich nuclei gives a natural explanation of the inversion of the even–odd effect. As we have already noted, if the mass number of a neutron-rich nucleus A is less than 250, the excitation energy of the daughter nucleus produced after β decay is less than the fission barrier and the neutron binding energy B_n. Therefore, delayed processes are either completely forbidden or have a low probability. Since the neutron-capture cross section of odd uranium isotopes is greater than for the even isotopes, the yield of even–even isotopes in the region $A < 250$ must be greater. This follows from the fact that for two neighboring nuclei in a neutron-capture chain the relation $N_1/N_2 = \sigma_2/\sigma_1$ holds in a first approximation; here, N_1 and N_2 are the numbers of nuclei with capture cross sections σ_1 and σ_2.

When delayed fission takes place with high probability, the losses in the chains of transformations with even A begin to be appreciable earlier than in the chains with odd A, since it is in these chains that one has odd–odd nuclei, for which the condition $Q_\beta > B_f$ begins to be satisfied in the first place; here Q_β is the β-decay energy of the parent odd–odd nucleus, and B_f is the fission barrier of the daughter nucleus. The calculation of the yield curves reveals a dependence of the inversion effect on the initial relative concentrations of the odd and even uranium isotopes, and also on the exposure nvt. At a higher exposure, the inversion effect occurs at higher A.

In the yield curve of the nuclei obtained from the HUTCH experiment, the "odd–even" inversion occurs at $A = 255$, whereas in the Par experiment the effect was observed at $A = 252$. Thus, the increase in the exposure from 7×10^{24} (the Par experiment) to 4.5×10^{25} neutron/cm^2 (the HUTCH experiment), the inversion effect was shifted by three or four units of the mass number to larger A.

A simple theoretical model including delayed processes enables one to predict not only the inversion effect but also the A region in which it occurs, depending on the exposure and the other initial conditions. The model adopted above provides a natural explanation of the absence of nuclei with $A > 258$ in the products of the thermonuclear explosions. This is explained by the circumstance that in the first stages of the β decay of the initial nuclei, for example, uranium, with mass number >257 there is intense emission of delayed neutrons. In addition, in the considered region the probabilities of delayed fission reach values of about 0.9. It should be noted that the element with atomic number 101 can be synthesized if uranium is irradiated and the mass number of the nucleus after the β-stability line has been reached is 259, and the element 102 can be synthesized when the mass number of the β-stable nucleus is 261.

Such values of the mass numbers and, therefore, the elements with $Z > 100$ can be obtained if neutron-rich isotopes of uranium with $A > 264$ are produced as a result of successive capture of neutrons. The chain of transformations with initial nucleus ^{264}U is shown in Fig. 20. It is characterized by a relatively uniform distribution of the nuclei over the even and odd masses, which comes about because of the (β^-, n), $(\beta^-, 2n)$, and $(\beta^-, 3n)$ reactions. An interesting feature of the calculation is the fact that the nuclei with high probability of delayed fission were found to be outside the main paths of the transformations, with the result that the losses due to delayed fission are only 4%. For "vertical" ascent in the hypothetical case when the emission of delayed neutrons is forbidden, almost 99% of the nuclei would be lost in the process of delayed fission.

It should be noted that an improved theoretical model is required to calculate the losses due to delayed fission, which are very sensitive to variations of the transformation paths of the initial nuclei. Therefore, the adopted average approach to the calculations of the losses due to delayed processes must be improved. However, the most important result of the calculations—the decrease in the mass number of the heaviest isotope which reaches the β-stability line by a few units compared with an initial nucleus with $A \approx 260$—is not in doubt. This means that the synthesis of β-stable isotopes in neutron pulses with $A \approx 260$ requires exposures that are orders of magnitude greater than those currently achieved.

5. DELAYED FISSION AND ASTROPHYSICAL PROCESSES OF HEAVY-ELEMENT SYNTHESIS

The duration of the neutron irradiation in the r process is such that β transformations of neutron-rich nuclei can take place as a result of neutron irradiation. Because of this, the probability of delayed fission occurs alongside the decay constants describing spontaneous fission and the emission of delayed neutrons in the astrophysical equations which describe the production of heavy nuclides in the neutron flux from supernovae.[56] It is obvious that delayed fission plays a part in the cooling of supernovae. It should be noted that at a definite stage delayed fission becomes the main energy source of a cooling neutron star. The nuclei synthesized in the r process with very large neutron excess and very large Q_β emit neutrons after β decay, although delayed fission is also energetically possible.

According to modern ideas, the decay of the neutron-rich nuclei produced in the neutron fluxes of the r process must take place in the following stages: Near the path of the r process, the main delayed process is the emission of neutrons; then, with decreasing neutron excess, delayed fission becomes more important than the emission of delayed neutrons, and when $Q_\beta < B_f$ there are competing processes—the emission of γ rays and delayed fission—and, finally, the daughter nuclei produced after β decay are de-excited by γ radiation.

Thus, the synthesis of a nucleus with mass number A depends in a complicated manner on the processes which take place in the chains of transformations of nuclei with $A+1, A+2, \ldots, A+n$.

In Refs. 12 and 41, estimates were made of the possible losses due to delayed fission in the β-transformation chains of heavy nuclei following neutron irradiation. In particular, special attention was paid to the stability region of nuclei with $A \approx 300$. The decrease in the relative yield of nuclei of the new stability region due to delayed fission was estimated to be between 2.6 and 190 for Z and A in the intervals 110–112 and 291–297, respectively, for surface-asymmetry constants 1.79 and 2.3 of the liquid-drop model.

The calculations made in Ref. 57 showed that if one takes into account the influence of delayed fission on the synthesis of heavy elements, the ratios of chronometric pairs, for example, $^{244}Pu/^{232}Th$, which govern our existing ideas about the rate and duration of nucleosynthesis, must be appreciably different from the values currently adopted.

CONCLUSIONS

The experimental and theoretical investigations of delayed fission took place in the following main stages.

The synthesis and study of nuclei that undergo delayed fission became possible when intense beams of multiply charged ions were achieved with the U-300 cyclotron and methods were developed for detecting fission fragments, in particular track detectors that are not sensitive to α particles.[1)]

As a result, in the first experiments[1-4] fragments were observed from the delayed fission of actinide nuclei with production cross section of about 10^{-34} cm^2 with a large yield, which clearly established the existence of delayed fission. Detection of fragments from delayed fission proved to be a good method of identifying new nuclei with large neutron deficit.

The study of the neutron-deficient Np and Am isotopes served as a stimulus for the theoretical prediction of possible A and Z regions in which delayed fission could be observed.[5,30]

In subsequent experiments, nuclei with very small production cross sections at the limit of the capabilities of modern experimental techniques were studied.[24,29] This led to the observation of delayed fission of neutron-deficient nuclei with $Z \geq 96$ (Ref. 29) and the neutron-rich Pa isotopes[32,34] at a short distance from the β-stability line. The obtained results were used to estimate the barriers of the studied nuclei under the assumption of a simple structure of the β-decay strength function.[26]

Accurate determination of the fission barriers from the data on delayed fission is only possible when allowance is made for the complicated low-lying structure of the β-decay strength function calculated by the "microscopic" method.[16] However, in some cases, for example, in the determination of the Z and A regions of delayed fission and calculations of deep below-barrier delayed fission, simple relations may be helpful.[29,40]

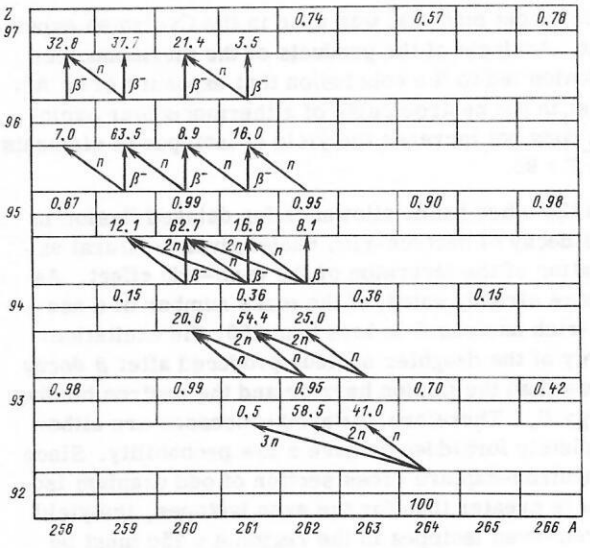

FIG. 20. Probability of delayed fission of neutron-rich nuclei (shown in the upper part of the squares for the parent nuclei) and the chain of transformations in the β decay of ^{264}U, including the emission of delayed neutrons. In the lower part of the squares, we give the fraction of nuclei which reach the given A and Z.

Development of the experimental investigations into the delayed fission of neutron-deficient nuclei requires a further increase in the intensity and selection of accelerated heavy ions, and also the use of new targets. Thus, it is now possible to make a detailed study of the α decay and x-ray emission after K capture of previously identified nuclei that undergo delayed fission. Of considerable interest is the possibility of investigating delayed processes of neutron-deficient nuclei with $N < 126$ in the region of Ra and Th.

A significant development in the experimental investigation of neutron-rich delayed emitters will be possible only with the creation of "clean" superpowerful neutron sources of the laser thermonuclear type.[57] However, many theoretical investigations into the delayed fission of neutron-rich nuclei have been made. These have shown that delayed fission has a significant influence on the yield of heavy nuclei in the synthesis of neutron-rich nuclei as well as in astrophysical nucleosynthesis processes. Further experimental study of the β-decay strength functions of neutron-rich nuclei will permit a fuller estimate of the part played by delayed fission in nucleosynthesis in high-intensity neutron fluxes.

I am very grateful to Academician G. N. Flerov and Yu. Ts. Oganesyan for their interest in the work, and to Yu. P. Gangrskiĭ for valuable comments and advice during the preparation of the review.

[1)] For a long time, virtually all experiments were made with the U-300 cyclotron at Dubna. It was only ten years later that results on the detection of delayed fission were repeated at Karlsruhe.[26]

[1]V. I. Kuznetsov, N. K. Skobelev, and G. N. Flerov, Yad. Fiz. **5**, 271 (1967) [Sov. J. Nucl. Phys. **5**, 191 (1967)].
[2]V. I. Kuznetsov, N. K. Skobelev, and G. N. Flerov, Yad. Fiz. **4**, 99 (1966) [Sov. J. Nucl. Phys. **4**, 70 (1967)].
[3]V. I. Kuznetsov, N. K. Skobelev, and G. N. Flerov, Yad. Fiz. **5**, 271 (1966) [Sov. J. Nucl. Phys. **5**, 191 (1966)].
[4]V. I. Kuznetsov, N. K. Skobelev, and G. N. Flerov, Yad. Fiz. **4**, 279 (1966) [Sov. J. Nucl. Phys. **4**, 202 (1967)].
[5]C. O. Wene and S. A. E. Johansson, in: Proc. Third Intern. Conf. on Nuclei Far from Stability, Report 76-13, CERN (1976), p. 21.
[6]N. K. Skobelev, Yad. Fiz. **15**, 444 (1972) [Sov. J. Nucl. Phys. **15**, 249 (1972)].
[7]V. E. Zhuchko *et al.*, Yad. Fiz. **28**, 1185 (1978) [Sov. J. Nucl. Phys. **28**, 611 (1978)].
[8]H. V. Klapdor *et al.*, Phys. Lett. **B78**, 20 (1978).
[9]A. M. Lane, A. G. Thomas, and E. P. Wigner, Phys. Rev. **98**, 693 (1955).
[10]C. L. Duke *et al.*, Nucl. Phys. **A151**, 609 (1970).
[11]V. A. Karnaukhov, Yad. Fiz. **10**, 450 (1969) [Sov. J. Nucl. Phys. **10**, 257 (1970)].
[12]K. Aleklett, G. Nyman, and G. Rudstam, Nucl. Phys. **A245**, 425 (1975).
[13]C. O. Wene and S. A. E. Johansson, Phys. Scr. **A10**, 156 (1974).
[14]H. V. Klapdor, Phys. Lett. **B65**, 5 (1976).
[15]C. O. Wene and H. V. Klapdor, in: Proc. Intern. Conf. on Nuclear Structure, Tokyo (1974), p. 797.
[16]I. N. Izosimov and Yu. V. Naumov, Izv. Akad. Nauk SSSR, Ser. Fiz. **42**, 2248 (1978).
[17]H. V. Klapdor *et al.*, Z. Phys. **A292**, 249 (1979).
[18]A. A. Bykov and Yu. V. Naumov, Izv. Akad. Nauk SSSR, Ser. Fiz. **42**, 1911 (1978).
[19]A. V. Ignatyuk, N. S. Rabotnov, and G. N. Smirenkin, Phys. Lett. **B29**, 200 (1969).
[20]C. Y. Wong and J. Bang, Phys. Lett. **B29**, 143 (1969).
[21]D. J. Hill and J. A. Wheeler, Phys. Rev. **99**, 1140 (1953).
[22]A. Gilbert and A. G. W. Cameron, Can. J. Phys. **43**, 1446 (1965).
[23]B. B. Back *et al.*, Phys. Rev. C **9**, 1924 (1974).
[24]Yu. P. Gangrskiĭ *et al.*, Preprint R7-12584 [in Russian], JINR, Dubna (1979), p. 6.
[25]V. S. Barashenkov and A. S. Iljinov, Nucl. Phys. **A206**, 131 (1973).
[26]D. Habs *et al.*, Z. Phys. **A285**, 53 (1978).
[27]L. P. Sommerville, M. I. Nurmia, and A. Ghiorso, in: Annual Report, Lawrence Berkeley Laboratory (1975), p. 39.
[28]L. Tommasino, N. Klein, and P. Solomon, Nucl. Track Detection 1, 63 (1977).
[29]Yu. P. Gangrskiĭ, M. B. Miller, and V. K. Utenkov, Preprint 13-12035 [in Russian], JINR, Dubna (1978).
[30]E. E. Berlovich and Yu. N. Novikov, Dokl. Akad. Nauk SSSR **185**, 1025 (1969) [Sov. Phys. Dokl. **14**, 351 (1969)].
[31]A. G. Belov *et al.*, Preprint R15-9795 [in Russian], JINR, Dubna (1976).
[32]Yu. P. Gangrskiĭ *et al.*, Yad. Fiz. **27**, 894 (1978) [Sov. J. Nucl. Phys. **27**, 475 (1978)].
[33]G. Wolzak and H. Morinaga, Radiochem. Acta **1**, 223 (1963).
[34]L. Kh. Batist *et al.*, Preprint [in Russian], Leningrad Institute of Nuclear Physics (1977), p. 363.
[35]W. D. Myers and W. J. Swiatecki, Nucl. Phys. **81**, 1 (1966).
[36]V. M. Strutinskiĭ, Yad. Fiz. **3**, 614 (1966) [Sov. J. Nucl. Phys. **3**, 449 (1966)]; Nucl. Phys. **A95**, 420 (1967); **A122**, 1 (1968).
[37]M. Brack *et al.*, Rev. Mod. Phys. **44**, 320 (1972).
[38]B. B. Back *et al.*, Phys. Rev. C **10**, 1948 (1974).
[39]Yu. Ts. Oganesyan, Preprint R9-12843 [in Russian], JINR, Dubna (1979), p. 17.
[40]V. I. Kuznetsov, Yad. Fiz. **30**, 321 (1979) [Sov. J. Nucl. Phys. **30**, 166 (1979)].
[41]P. Moller and J. R. Nix, in: IAEA Third Symposium on the Physics and Chemistry of Fission, Vol. 1, Rochester (1973), p. 103; Nucl. Phys. **A229**, 269 (1974).
[42]H. C. Pauli, Phys. Rev. **7**, 35 (1973).
[43]S. E. Larsson and G. Leander in: Ref. 41, p. 177.
[44]V. V. Pashkevich, Nucl. Phys. **A133**, 400 (1969).
[45]K. L. Kratz *et al.*, Phys. Lett. **B65**, 231 (1976).
[46]K. L. Kratz *et al.*, Nucl. Phys. **A317**, 335 (1979).
[47]P. Glassel, H. Rosler, and H. J. Specht, Nucl. Phys. **A256**, 220 (1976).
[48]Yu. Ts. Oganesyan, V. I. Kuznetsov, and Yu. A. Lazarev, in: Mezhdunarodnyĭ simpozium po sintezu i svoĭstvam novykh élementov (Intern. Symposium on Synthesis and the Properties of New Elements), D7-80-556, JINR, Dubna (1980), p. 52.
[49]J. S. Ingley, Nucl. Phys. **A124**, 130 (1969).
[50]G. A. Cowan, in: R. A. Welch Foundation Conferences on Chemical Research, Vol. 13, Houston, Texas (1969), p. 291.
[51]S. A. E. Johansson and C. O. Wene, Ark. Fys. **36**, 353 (1967).
[52]P. Moller and J. R. Nix, in: Ref. 41, p. 10.
[53]I. G. Bell, in: Intern. Conf. on the Study of Nuclear Structure with Neutrons, Antwerp, July (1965), p. 127.
[54]D. W. Dorn and R. W. Hoff, Phys. Rev. Lett. **14**, 440 (1965).
[55]T. Ohnishi, Appl. Space Sci. **58**, 149 (1978).
[56]C. O. Wene, Astron. Astrophys. **44**, 233 (1975).
[57]H. V. Klapdor and C. O. Wene, MPIH-1979, Vol. 13, p. 91.

Translated by Julian B. Barbour